



# Thrust Faults Promoted Hydrocarbon Leakage at the Compressional Zone of Fine-Grained Mass-Transport Deposits

Qiliang Sun<sup>1,2\*</sup>, Xinong Xie<sup>1</sup>, Shiguo Wu<sup>3</sup> and Guorui Yin<sup>4</sup>

<sup>1</sup>Hubei Key Laboratory of Marine Geological Resources, China University of Geosciences, Wuhan, China, <sup>2</sup>Laboratory for Marine Mineral Resources, Qingdao National Laboratory for Marine Science and Technology, Qingdao, China, <sup>3</sup>Laboratory of Marine Geophysics and Georesource, Institute of Deep-sea Science and Engineering, Chinese Academy of Sciences, Sanya, China, <sup>4</sup>PetroChina Changqing Oil Field Company, Xian, China

## OPEN ACCESS

### Edited by:

Adam McArthur,  
University of Leeds, United Kingdom

### Reviewed by:

Xishuang Li,  
Ministry of Natural Resources, China  
Nan Wu,  
Tongji University, China

### \*Correspondence:

Qiliang Sun  
sunqiliang@cug.edu.cn

### Specialty section:

This article was submitted to  
Sedimentology, Stratigraphy and  
Diagenesis,  
a section of the journal  
Frontiers in Earth Science

**Received:** 25 August 2021

**Accepted:** 15 October 2021

**Published:** 17 November 2021

### Citation:

Sun Q, Xie X, Wu S and Yin G (2021)  
Thrust Faults Promoted Hydrocarbon  
Leakage at the Compressional Zone of  
Fine-Grained Mass-  
Transport Deposits.  
*Front. Earth Sci.* 9:764319.  
doi: 10.3389/feart.2021.764319

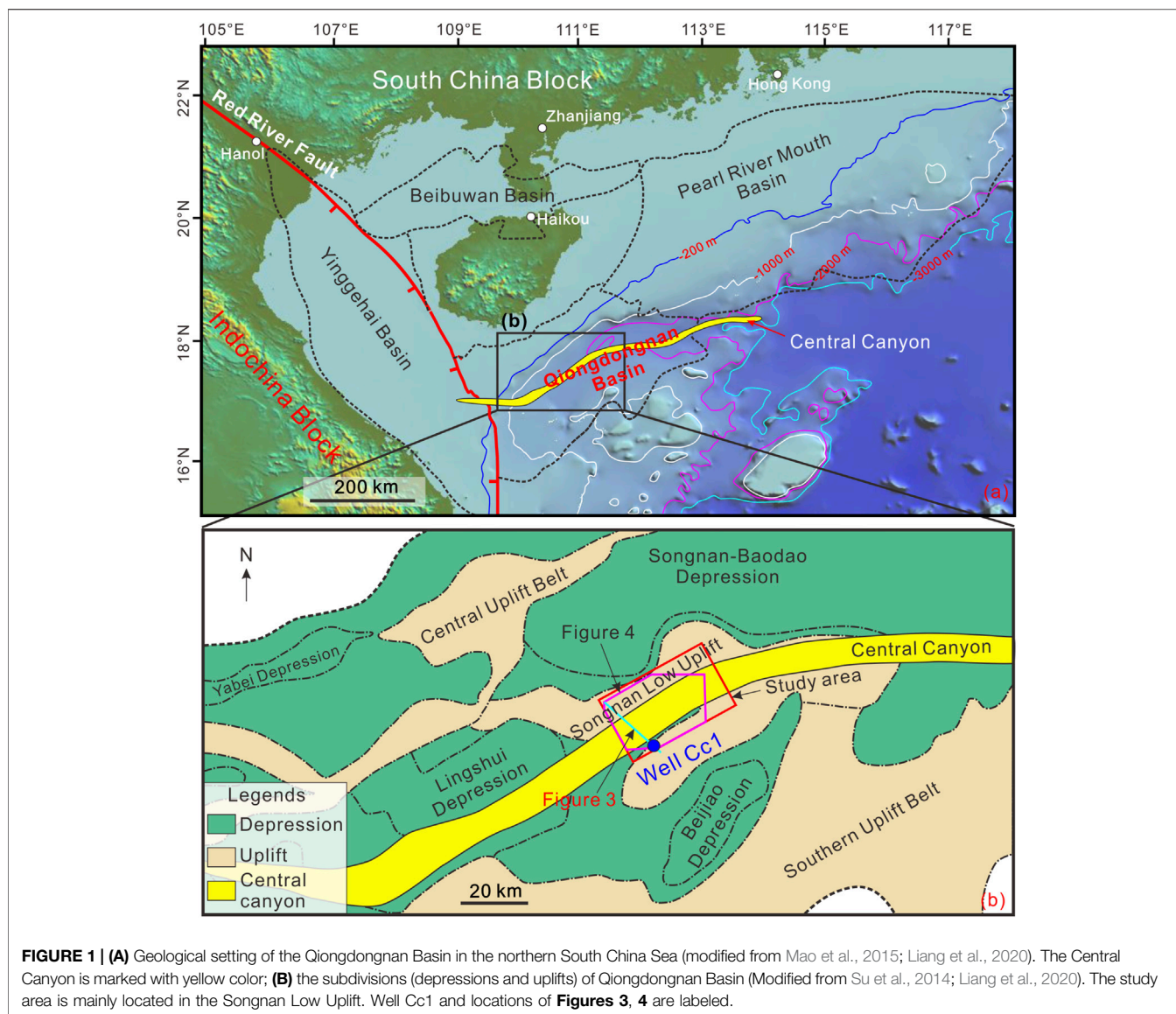
Fine-grained mass-transport deposits (MTDs), especially their compressional toe zones, are traditionally considered as effective seal in constraining the vertical fluid migration underneath. However, this study documents thrust faults at the compressional toe zone of fine-grained MTDs that could disaggregate the seal competence and promote vertical fluid flow. The investigated MTD referred to as MTD-a lies directly over a large hydrocarbon reservoir that is located within the Central Canyon of northern South China Sea, which is examined by using high-resolution 3D seismic and borehole data. Thrust faults and irregular blocks composed of coarse-grained sandstones are observed in the compressional zone of the MTD-a's toe. More importantly, seismic evidence (e.g., enhanced seismic reflections) suggests that a large amount of hydrocarbons from the underlying reservoir penetrated through the MTD-a along these thrust faults and charged into the coarse-grained sandstone blocks. This clear evidence of thrust faults compromising the MTD's seal effectiveness and thus facilitating the vertical fluid flow through the non-permeable strata demonstrate the importance of reassessing the seal capacity of MTD.

**Keywords:** mass-transport deposits, thrust fault, hydrocarbon leakage, block, South China Sea

## INTRODUCTION

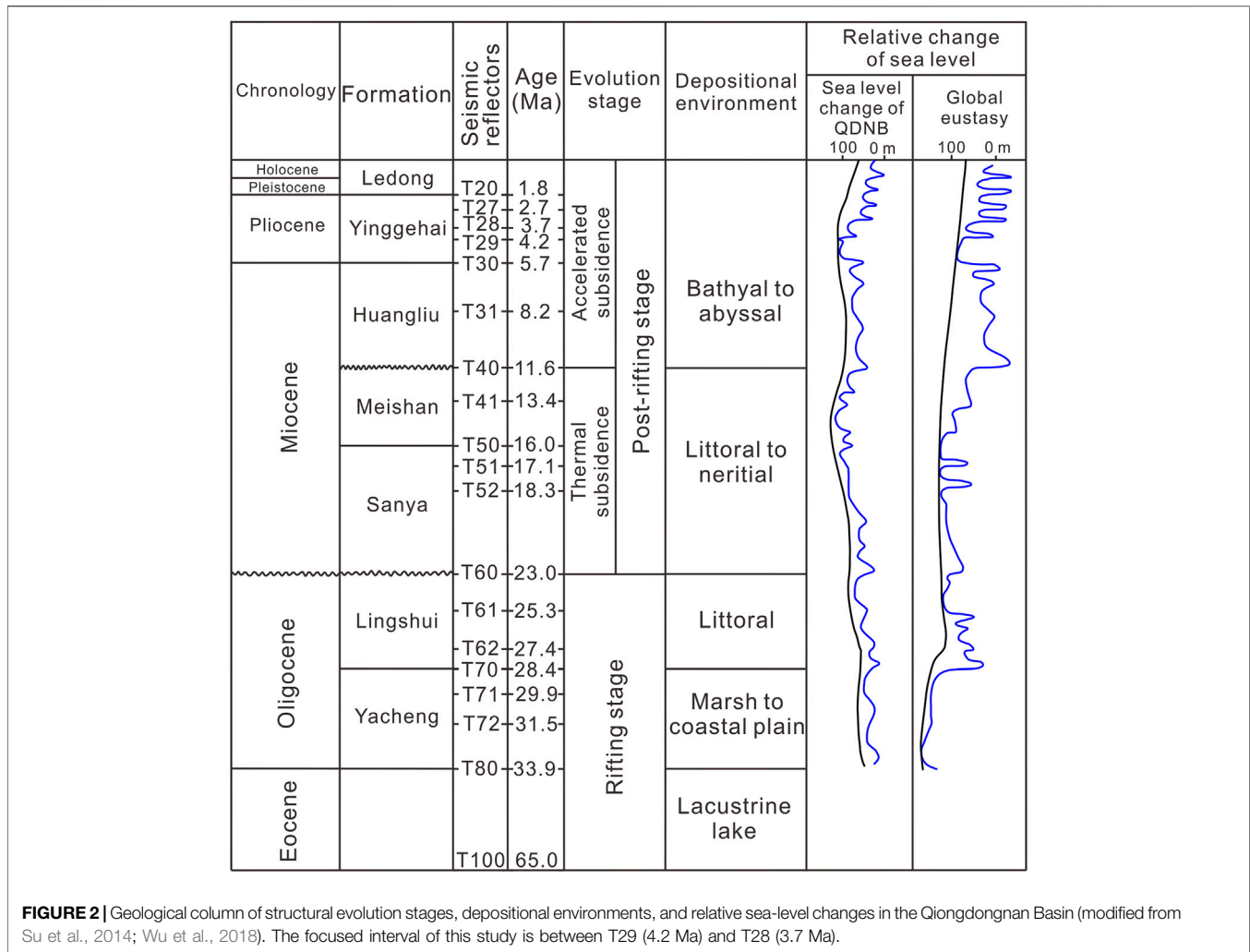
Mass-transport deposits (MTDs) widely occur at the continental margins and island flanks. They are usually composed of the headwall domain, translational domain, and toe domain (Martinsen, 1994; Lastras et al., 2002) and, accordingly, a systematic distribution of strain transferred from extensional structures in the headwall zone to compressional structures in the toe zone (Trincardi and Argnani, 1990; Canals et al., 2004; Frey Martinez et al., 2005). Thrust faults are an important component of MTDs at their compressional toe zones (Bull et al., 2009; Ogata et al., 2014; Alsop et al., 2017). They are usually caused by the translating material buttressing against a seabed obstacle (Lewis, 1971; Moscardelli et al., 2006) and typically affect the entire thickness of the MTD (Frey Martinez et al., 2005; Bull et al., 2009).

Thrust faults are mainly imaged by geophysical data (e.g., seismic reflection data) and shown as imbricated structures (Lamarche et al., 2008; Lackey et al., 2018). Because of the shear compaction and dewatering during the mass movement (e.g., decreases of porosities and permeability), MTDs,



especially those mainly composed of unlithified fine-grained sediments, are proposed as seal/barrier for the vertical fluid flow (Dugan, 2012; Alves et al., 2014; Sun and Alves, 2020). Furthermore, failed sediments are inclined to accumulate and thus thicken at the compressional toe zones (Moscardelli et al., 2006; Lamarche et al., 2008). Furthermore, the long-distance transportation of failed sediments at the toe zone is typically highly deformed and thus their fabrics are greatly damaged. These make the seal capacity of compressional toe zones of MTDs more effective. Although remnant blocks within MTDs are proposed to provide conduits for the vertical fluid flows (Alves et al., 2014; Gamba and Alves, 2015; Cox et al., 2020), no vertical flow pathways have been identified at the compressional toe zone until now.

In this study, the investigated MTD, here referred to as MTD-a, is immediately lying on a large hydrocarbon reservoir in the Qiongdongnan Basin (QDNB) of the northern South China Sea, based on high-resolution 3D seismic and borehole data. The aims of this study are 1) to characterize the MTD-a, including the internal structures, blocks, and free gas within the MTD-a; 2) to assess the seal completeness of the compressional zone of MTD-a; and 3) to explore the vertical fluid migration system in the study area. This study demonstrates that free gas has leaked from the underlying hydrocarbon reservoir and migrated into the blocks through thrust faults. Therefore, it provides clear evidence for the thrust faults at the compressional zone of MTDs serving as fluid pathways for the first time, which suggests that the seal completeness of MTDs should be reassessed where the thrust faults develop.



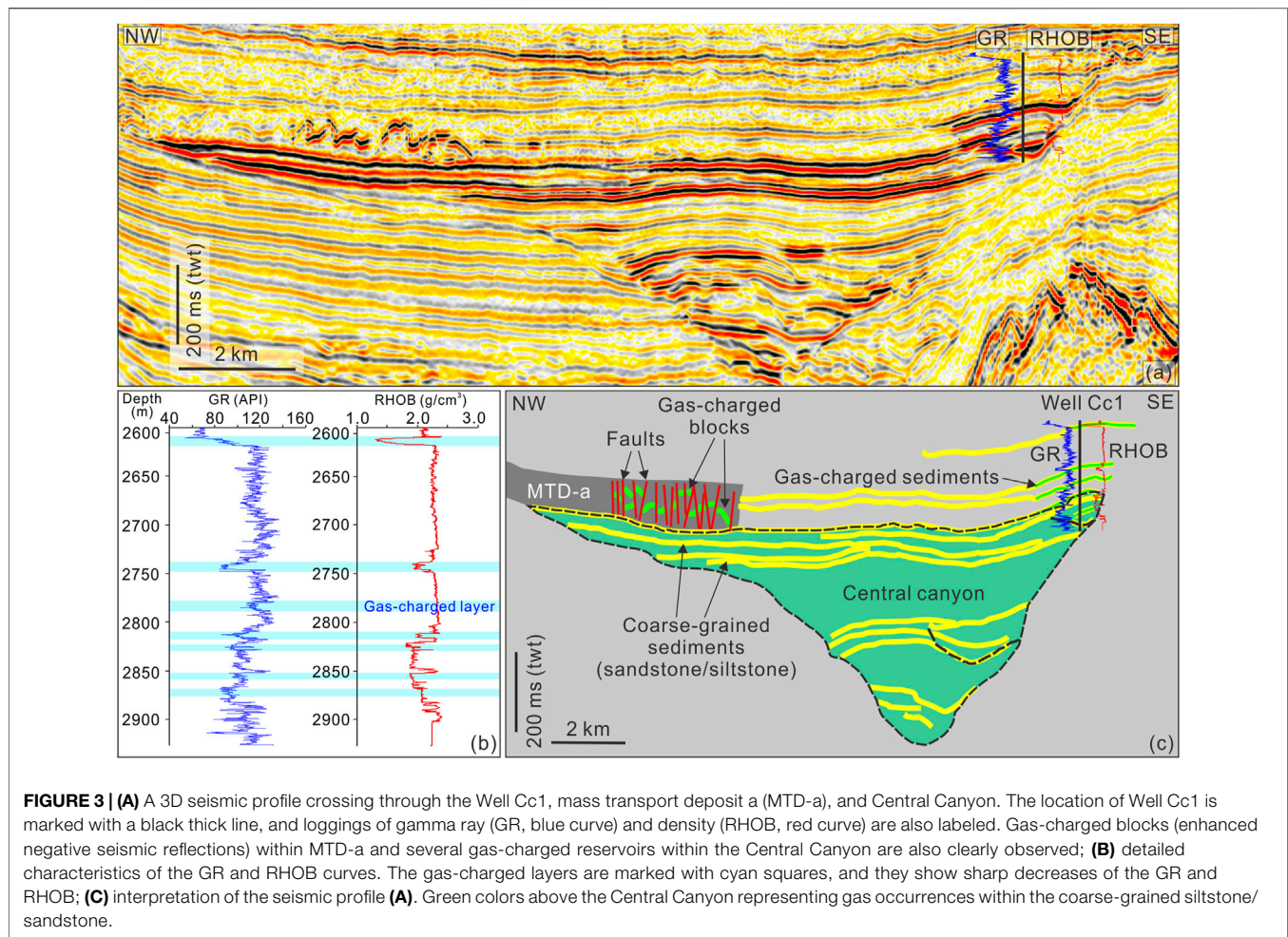
## GEOLOGICAL SETTING

The QDNB, one of the Cenozoic basins in the northern South China Sea located to the southeast of Hainan Island (**Figure 1**), covers an area of ~45,000 km<sup>2</sup> (Xie et al., 2008; Su et al., 2014). It comprises a few uplifts (massifs) and depressions (sags) (**Figure 1B**). The QDNB formed through two-stage tectonic evolutions, the Eocene-Oligocene rifting stage and the Miocene-to-Present post-rifting stage (**Figure 2**) (Gong and Li, 1997; Wu et al., 2008). During the rifting stage, deposits from the marsh-to-coastal plain Yacheng Formation and the littoral Lingshui Formation formed the main source rocks in the QDNB (Zhu et al., 2009). The post-rifting strata are composed of the littoral to neritic Sanya and Meishan formations, as well as the bathyal to abyssal Huangliu, Yinggehai, and Ledong formations (**Figure 2**) (Gong and Li, 1997; Zhu et al., 2009).

The QDNB is petroliferous, especially along the axis of the Central Canyon where numerous hydrocarbon fields have been found (Zhu et al., 2009; Wang Z. et al., 2015; Chen et al., 2015). The Central Canyon is > 425 km long and 3–16 km wide (Su

et al., 2014). Its deep incision into the strata as old as 8.2 Ma was fully filled at ~4.2 Ma (Liang et al., 2020). Moreover, the Central Canyon is mainly filled by the fine-grained mudstone and layered coarse-grained sandstone that acts as hydrocarbon reservoir (Wang Z. et al., 2015). After ~4.2 Ma, multiple MTDs are draped on the Central Canyon strata and formed the seal for the hydrocarbon reservoir (Liang et al., 2020).

MTDs widely developed in the QDNB and those in the southern QDNB (Huaguang Sag) are well studied (Sun et al., 2011; Wang et al., 2013; Wang D. et al., 2015). Those MTDs are cyclic with turbidities, such as triple packs of turbidities and MTDs, which are probably related to the sea-level changes (Sun et al., 2011). Moreover, the reactivation of major faults and associated volcanism in the late Miocene were proposed as the dominant trigger mechanisms for those MTDs (Wang et al., 2013). MTDs also frequently occurred in the central QDNB, as mentioned above (Liang et al., 2020). They may source from the northern slope area, western slope area, or Guangle Massif (Cheng et al., 2021) and mainly formed after ~4.2 Ma (Liang et al., 2020). Moreover, the slope overstepping



resulting from high sediment supply likely triggered the slope instability (Qin et al., 2015; Liang et al., 2020). The occurrence of MTDs greatly changed the sediment dispersal pattern in the Central Canyon and thus influenced the hydrocarbon systems (reservoirs and seals) in the study area (Li et al., 2015; Liang et al., 2020).

## DATA AND METHODS

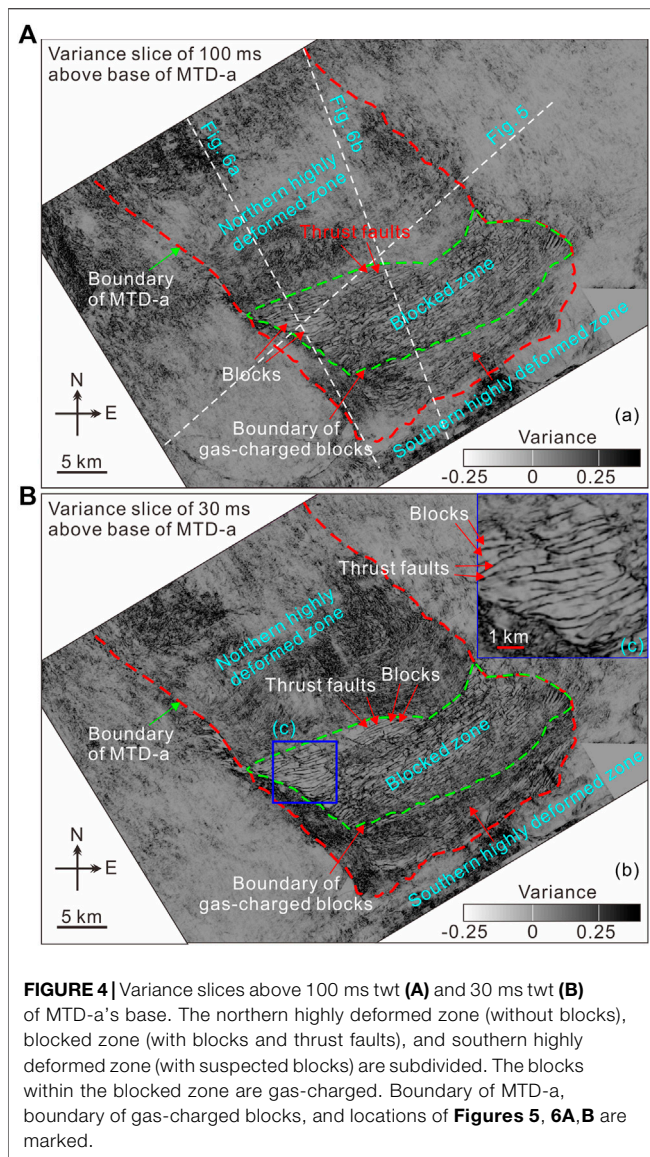
The time-migrated 3D seismic reflection data used in this study cover an area of  $\sim 1,050 \text{ km}^2$  and were provided by the China National Offshore Oil Corporation (CNOOC). It was acquired in 2010 with 3,000-m-long streamers consisting of 240 channels at a spacing of 12.5 m and a sample rate of 4 ms. The bin spacing of the 3D seismic data is 25 m in the crossline and 12.5 m in the inline. The dominant frequency of the focused strata is  $\sim 35 \text{ Hz}$ , and thus, a vertical resolution of  $\sim 20 \text{ m}$  is calculated, based on the strata velocity of 2,800 m/s from the Well Cc1 (Figure 1B). The 3D seismic reflection data are zero-phase processed and displayed with the Society of Exploration Geophysicists (SEG) normal polarity, whereby a downward increase in acoustic

impedance corresponds to a positive reflection event (red on seismic profiles) (Brown, 2004). Exploration well Cc1 is used for the lithology and strata velocity correlation. This well was located at the flank of the Central Canyon and drilled through several gas-charged sandstone layers (Figure 3). To better image the blocks, a variance attribute is used in this study (Figure 4). The variance attribute measures the variability in shape between seismic traces (Brown, 2004). It is directly derived from the processed data and thus is free of interpreter bias. The variance attribute is typically used to map structural and stratigraphic discontinuities (e.g., blocks, faults, and channels).

## RESULTS

### General Characteristics

The most prominent structure in the study area is the “V”-shaped Central Canyon. It quickly widens upward, and the fill sediments onlap onto its walls (Figures 3A,C, 6). The strata are mainly parallel/subparallel along the axis of the Central Canyon (Figure 5), and tapering/onlapping seismic



reflections are only occasionally observed along the axis (**Figure 5**). Many boreholes have targeted the hydrocarbon-rich Central Canyon and show that the strata mainly comprise fine-grained mudstone (Su et al., 2014; Liang et al., 2020). Coarse-grained siltstone and sandstone are also observed within the Central Canyon (**Figure 3C**), which is the main hydrocarbon reservoir (Wang Z. et al., 2015).

Multiple MTDs characterized by chaotic/blanking seismic reflections are observed above the Central Canyon, separated by continuous seismic surfaces (**Figures 3A, 5, 6**). This study is focused on the lowermost MTD, here named as MTD-a, which is directly draped on the Central Canyon (**Figure 3A**).

Many irregular blocks, characterized by short enhanced-amplitude, negative-polarity seismic reflections are identified inside the MTD-a (**Figures 3A, 5–7**). Although there is no well directly through these blocks, referencing the Well Cc1's layered

structure leads to a reasonable assumption that the blocks are mainly composed of sandstones (**Figure 3**). The blocks are surrounded by fine-grained mudstone (chaotic seismic reflections). The head zone of MTD-a has not been imaged, because of the limitation of 3D seismic coverage (**Figure 4**). It may have originated from the slope of QDNB to the north (**Figure 1**) and flowed toward the southeast part, judging from the extension of MTD-a (e.g., the direction of the lateral margins) (**Figure 4**). In the 3D seismic coverage, MTD-a could be divided into three subzones, such as a northern highly deformed zone, a blocked zone, and a southern highly deformed zone (**Figure 4**). No macroscopic blocks could be observed within the northern highly deformed zone, and it is mainly composed of chaotic seismic reflections (**Figure 6**). In the blocked zone, blocks float within the fine-grained strata (mudstone) and they are separated by high-angle thrust faults (**Figure 5**). There are suspected blocks observed on the variance slices in the highly deformed zone to the south (**Figure 4**). However, the seismic identification of these structures is not definitive (**Figures 3A, 6**).

## Blocks

A total of 306 seismic-scale irregular blocks were recorded in the study area, characterized by enhanced seismic reflections as mentioned above, and are observed in the toe zone of MTD-a, especially those close to the southeastern boundary (blocked zone; green dashed zones in **Figure 4A**). However, the blocks are rarely observed at the distal termination part of MTD-a (southern highly deformed zone; **Figure 4A**). They are mainly bounded by thrust faults to their northwestern and southeastern sides and surrounded by chaotic seismic reflections (**Figures 6, 7**). In other words, they “float” within the chaotic seismic reflections. Although they are bounded by the thrust faults, the blocks are close to each other and some of them are even directly connected (**Figure 7**).

The irregular blocks are distributed in a linear fashion in plain view with orientations of E–W at the northwestern corner of the blocked zone and NE–SW at the left blocked zone (**Figure 4**). The dips of blocks are perpendicular to their strike extensions, and a few blocks are nearly horizontal elongation without any dips (**Figure 5**). The lengths of blocks range from ~0.20 to ~6.34 km with an average of ~1.48 km, while the blocks' widths are between ~0.10 and ~2.05 km, with an average of ~0.27 km. There is no apparent relationship between the lengths and widths of blocks ( $R^2 = 0.03$ ; **Figure 8A**). The blocks cover an average area of ~0.44 km<sup>2</sup> ranging from ~0.02 to ~4.24 km<sup>2</sup>. The areas of blocks are moderately related to their lengths ( $R^2 = 0.54$ ; **Figure 8B**) and widths ( $R^2 = 0.50$ ; **Figure 8C**). The average height of blocks is ~42.4 m (~30.3 ms twt), and thus the total volume of blocks (total area × average height) is ~5.68 km<sup>3</sup>.

## Thrust Faults

A total of 350 seismic-scale thrust faults are identified in the blocked zone, which separate the blocks apart (**Figures 5, 7**).

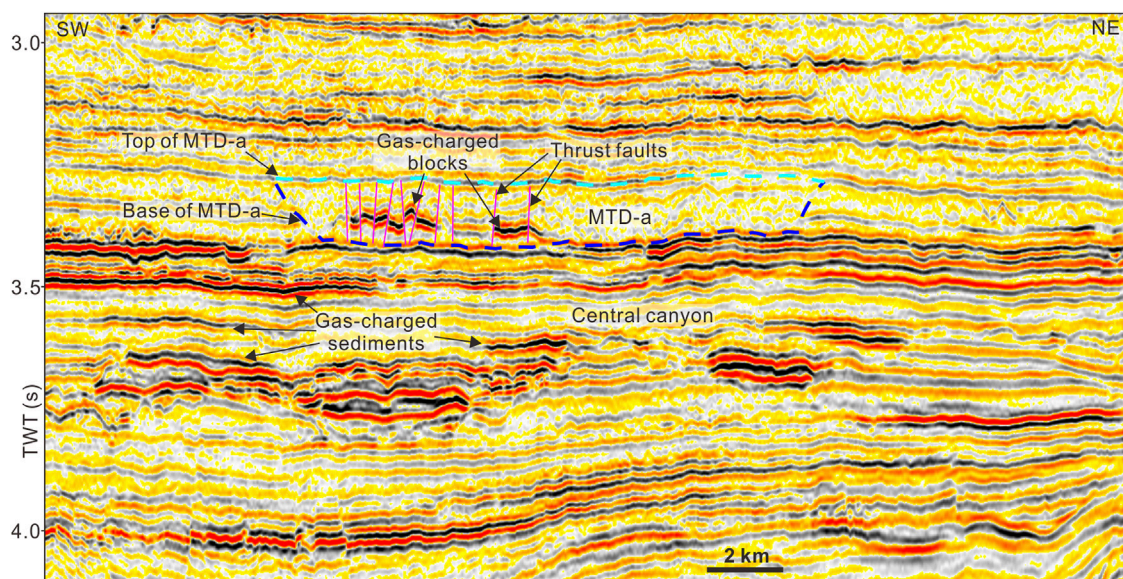


**FIGURE 5** | A 3D seismic profile perpendicular to the extension of MTD-a shows its lateral boundaries. Gas-charged blocks are clearly observed within MTD-a. Central Canyon is mainly unfilled by layered sediments. Top and base of MTD-a are marked with cyan and blue dashed lines. See location in **Figure 4**.

Most of the thrust faults penetrate the whole MTD-a and terminate at the upper surface of the underlying Central Canyon strata (**Figure 6**). However, some small-scale thrust faults are mainly located in the upper part (above the blocks) of MTD-a (**Figure 7B**). The lengths of thrust faults range between ~0.27 and ~4.92 km with an average of ~1.4 km (**Figure 8D**). The strikes of thrust faults mainly extend between 40° and 70° (~84% of the total thrust faults) (**Figure 8D**). Less thrust faults strike 90°–147°, and they usually have short vertical extensions (<1.0 km; **Figure 8D**). Accordingly, the thrust faults mainly incline 130°–160° (37% of the total thrust faults) and 320°–340° (45% of the total thrust faults; **Figure 8E**). The dips of thrust faults range from ~25° to ~87°, and most of them (90%) are between ~30° and ~70° (**Figure 8F**).

## Free Gas

Enhanced seismic anomalies characterized by negative reflections are observed in the Central Canyon and MTD-a's blocks (**Figures 3A, 5–7**), which is similar to the typical seismic characteristics of free gas (e.g., Judd and Hovland, 2007; Løseth et al., 2009; Sun et al., 2017). In fact, the exploration well Cc1 drilled through these enhanced seismic anomalies and confirmed that they are gas-charged sandstones (**Figures 3A,C**). Furthermore, these gas-charged sandstones characterized by sharp decreases of gamma ray (GR) and density (RHOB) are surrounded by fine-grained mudstones (**Figure 3B**). Accordingly, the irregular blocks within MTD-a could be interpreted as the counterparts of sandstones (**Figure 3C**). Moreover, the enhanced negative seismic reflections of blocks (**Figures 3A, 5–7**) indicate that free gas also charged into them. The average porosity of sandstone from well Cc1 is ~29.6%, and that of gas saturation

is ~71.2%; hence, the volume of free gas stored within the MTD-a' blocks can be as high as  $\sim 1.2 \times 10^9 \text{ m}^3$ .

## DISCUSSION

### Seal Disintegration and Vertical Hydrocarbon Migration

Fine-grained MTDs usually have decreased porosities and permeability, because of shear compaction and dewatering during their emplacement (Piper et al., 1997; Shipp et al., 2004; Sawyer et al., 2007; Dugan, 2012; Sun and Alves, 2020). Therefore, they usually act as effective seal to hinder the vertical migration of fluids (Alves et al., 2014; Sun and Alves, 2020). Remnant blocks that break through the MTDs could occasionally support the vertical fluid migration (Gamboa and Alves, 2015; Cox et al., 2020). However, there are no reports about vertical fluid flow in the compressional toe zone of MTDs as yet, where the compressional stress in the toe zone is proposed to strengthen the seal capacity of sediments.

Gas-charged blocks within MTD-a indicate that significant amounts of hydrocarbon have leaked from the gas field underlying the MTD-a (**Figures 5–7**). Because the blocks are surrounded by fine-grained sediments and are not directly connected with the underlying gas reservoir, the thrust faults are believed to act as the primary pathways for vertical fluid migration. Normally, the thrust faults in the compressional environment would be tight/closed to barrier fluids (Elmore et al., 2003; Micklethwaite, 2008). However, the thrust faults, likely with fractured medias, are mechanically weak zones (e.g., Lacroix et al., 2014; Cook et al., 2020), and they would likely reactivate under overpressure due to the underlying

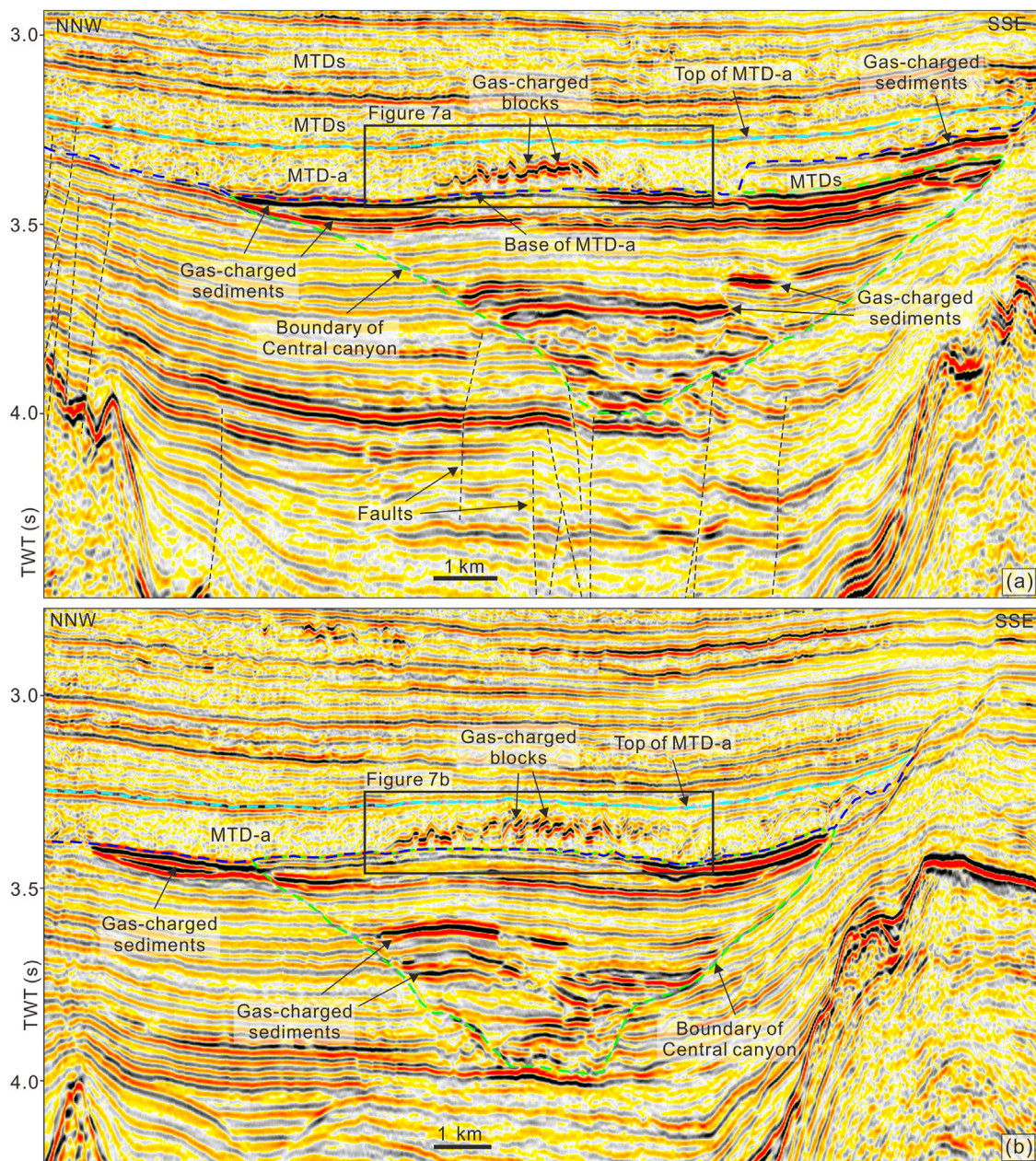


**FIGURE 6** | 3D seismic profiles nearly parallel to the extension of MTD-a. MTD-a directly overlies the Central Canyon. Several gas-charged layers (enhanced negative seismic reflections), especially the uppermost layers, occurred within the Central Canyon. Gas-charged blocks within the MTD-a are surrounded by chaotic seismic reflections, interpreted as mudstone. Normal faults developed below the Central Canyon, and they provide the main pathways for the deep-seated hydrocarbon migration. Locations of **Figures 7A,B** are marked with black squares.

accumulation of hydrocarbons. Moreover, the blocked zone has weaker deformation compared to the northern and southern highly deformed zones where the failed sediments are probably fully mixed (**Figure 4**). The less mixture of sediments in the blocked zone would partly keep the fabrics of the strata, which is also in favor of reactivation of the thrust faults. This study documents the thrust faults at the compressional zone of MTDs to serve as fluid pathways for the first time. It also indicates that the fabric heterogeneity plays an important role

on the seal completeness, and certain factors (e.g., overpressure) may trigger the disintegration of seal, even for the fine-grained sediment-dominated compressional zones of MTDs.

## Hydrocarbon Migration and Accumulation System

The hydrocarbon migration and accumulation system in the study area can be updated through this study together with

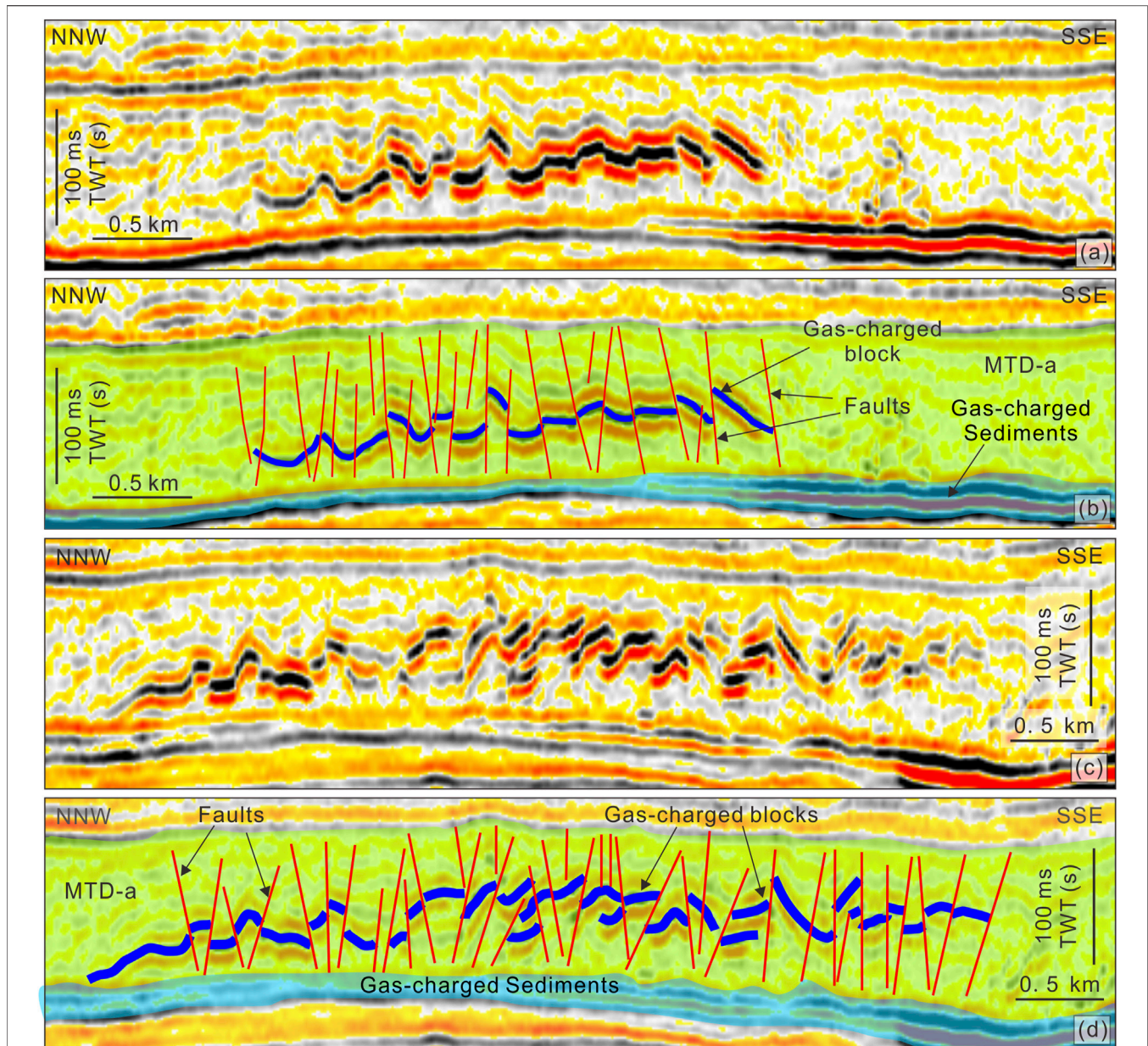
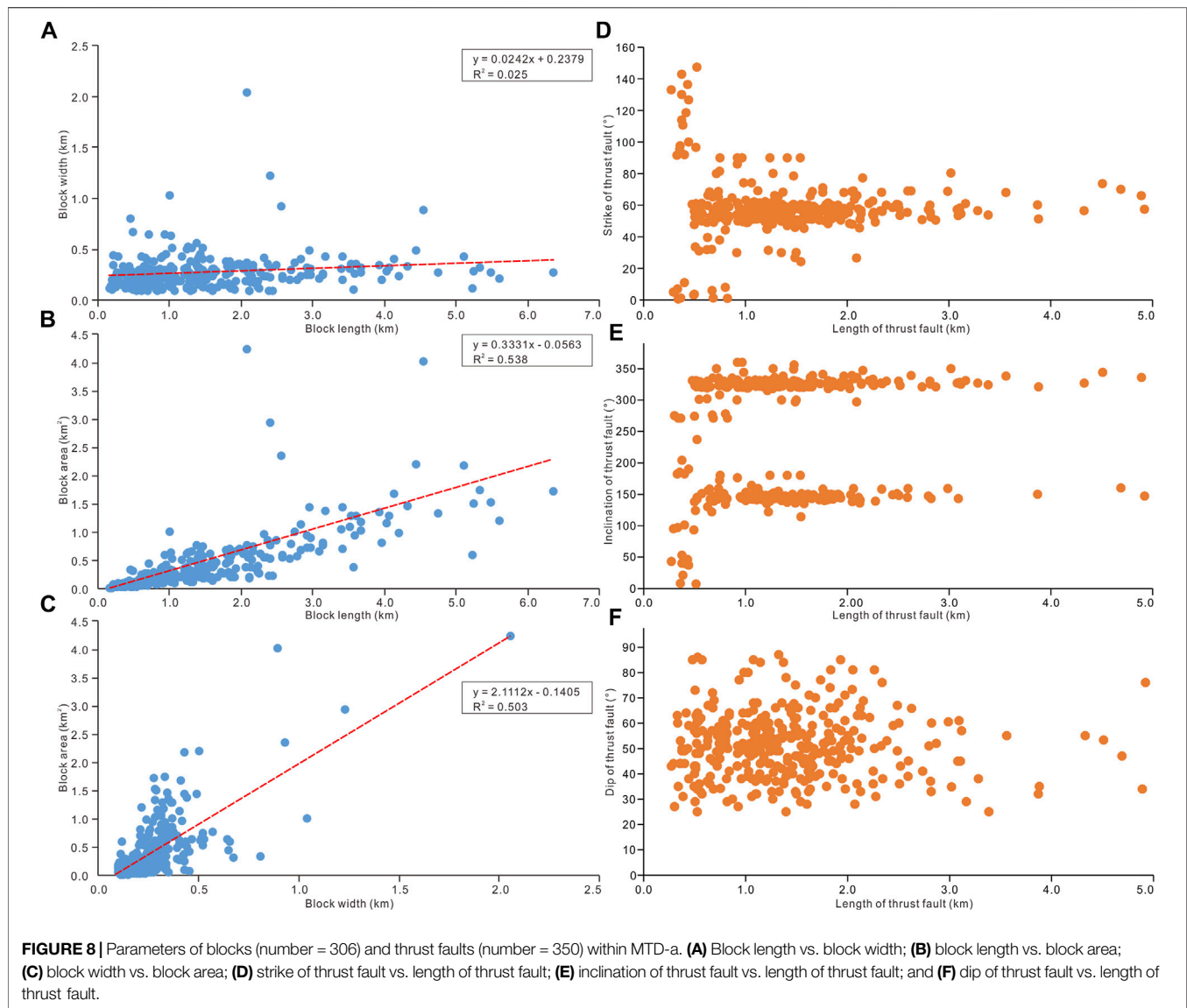


**FIGURE 7 |** Enlargements of seismic profiles **(A,C)** and their interpretation **(B,D)** showing the details of blocks and thrust faults within MTD-a. MTD-a directly lies on the hydrocarbon reservoir. Thrust faults link the underlying hydrocarbon reservoir and MTD-a' blocks and provide pathways for the gas leaking upward.

previous studies (Zhu et al., 2009; Li et al., 2017). The deeply buried coal-bearing strata of the lower Oligocene Yacheng Formation serve as the main source rock in the QDNB (Huang et al., 2003). The source rock entered the peak gas-generation window during the late Miocene and Pliocene (Zhu et al., 2009). Hydrocarbon (gas) from the source rock migrated upward mainly along tectonic faults (Figure 6A) and charged into the reservoir of the Central Canyon from the Pliocene to the present (Wang et al., 2014). Within the Central Canyon, the interconnected coarse-grained siltstone/sandstones provided

the lateral and vertical hydrocarbon migration pathways (Figure 9). Finally, the hydrocarbon accumulated at the topmost part of the Central Canyon where the reservoir is directly capped by the compressional zone of the fine-grained MTD-a (Figures 6, 9). The compressional zone of MTD-a is composed of a series of thrust faults and coarse-grained blocks, as mentioned above (Figure 3). Accompanying the gradual accumulation of hydrocarbon, overpressure would increase and finally exceed the yield strength of thrust faults. Therefore, the thrust faults would reactivate and allow



hydrocarbons would migrate upward along these faults and charge the blocks, as observed in this study (Figures 7, 9). This study indicates that a large amount of hydrocarbons ( $\sim 1.2 \times 10^9 \text{ m}^3$ ) has probably leaked from the main reservoir of the gas field. Furthermore, the hydrocarbon system including the hydrocarbon migration, accumulation, and leakage in the study area is probably still dynamic, and special attention should be paid to the seal completeness where thrust faults occur within the MTDs.

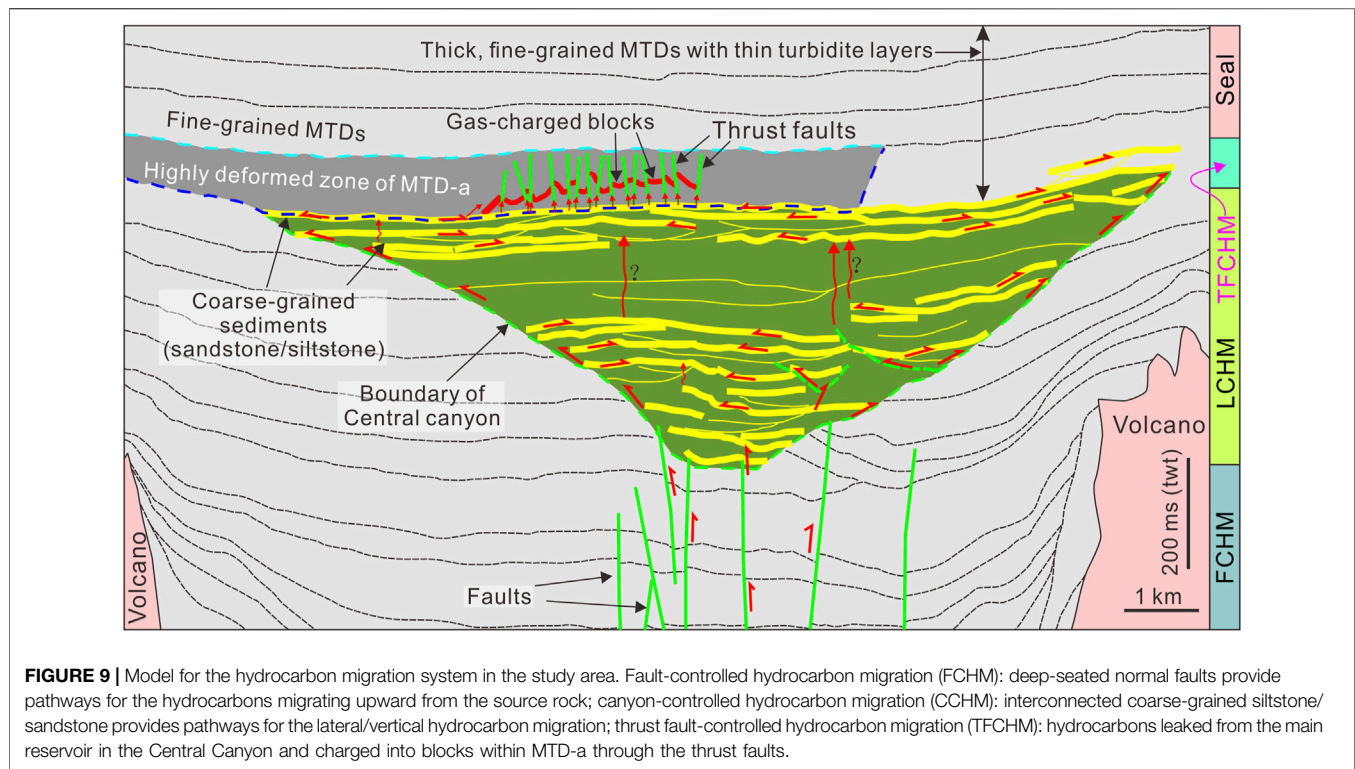
## CONCLUSION

This paper is focused on an MTD-a that is directly overlying a large gas field in the Central Canyon of the Qiongdongnan Basin (South China Sea), using high-resolution 3D seismic

data and borehole data. The main conclusions are drawn as follows:

- 1) Well-developed seismic-scale blocks and thrust faults are widespread in the compressional zone of MTD-a.
- 2) Thrust faults helped to penetrate MTD-a's seal and provided pathways for vertical fluid migration. This is the primary mechanism for as much as  $1.2 \times 10^9 \text{ m}^3$  of hydrocarbon to escape from the reservoir, migrate upward, and eventually accumulate in the sandstone blocks.

This study provided clear evidence for the thrust faults promoting fluid flow at the compressional zone of MTDs for the first time, which has important implication on the assessment of MTDs' seal competence and underlying reservoir completeness. Moreover, reevaluation of other fine-grained



MTDs assumed as seals is advised to reduce uncertainty in the sealing capacity of MTDs, particularly those displaying blocky and faulted textures.

## DATA AVAILABILITY STATEMENT

The original contributions presented in the study are included in the article/Supplementary Material, further inquiries can be directed to the corresponding author.

## AUTHOR CONTRIBUTIONS

QS is the principal author and primary seismic interpreter, and also writes and edits the paper. XX and SW contribute on the interpreting the seismic data, and writing/editing the paper. GY contributes on preparing the figures and writing the paper.

## REFERENCES

- Alsop, G. I., Marco, S., Levi, T., and Weinberger, R. (2017). Fold and Thrust Systems in Mass Transport Deposits. *J. Struct. Geology*, 94, 98–115. doi:10.1016/j.jsg.2016.11.008
- Alves, T. M., Kurtev, K., Moore, G. F., and Strasser, M. (2014). Assessing the Internal Character, Reservoir Potential, and Seal Competence of Mass-Transport Deposits Using Seismic Texture: A Geophysical and Petrophysical Approach. *Bulletin* 98, 793–824. doi:10.1306/09121313117

## FUNDING

This work was supported by the National Key R&D Program of China (No. 2018YFC0310000), the National Scientific Foundation of China (No. 41676051), and the Fundamental Research Funds for the Central Universities-the China University of Geosciences (Wuhan) (No. CUG2106207).

## ACKNOWLEDGMENTS

The China National Offshore Oil Company (CNOOC) is thanked for permission to release the data. The data that support the findings of this study are available from the CNOOC. Restrictions apply to the availability of these data, which were used under license for this study. Prof. Jingping Xu is thanked for his constructive comments on the original version of this paper. Guest Editor AM, Reviewer NW and an reviewer are thanked for their constructive comments that greatly improved this paper.

- Brown, A. R. (2004). Interpretation of Three-Dimensional Seismic Data: AAPG Memoir 42, in *SEG Investigations in Geophysics*. 6th Edn. Tulsa: The American Association of Petroleum Geologists and the Society of Exploration Geophysicists.
- Bull, S., Cartwright, J., and Huuse, M. (2009). A Review of Kinematic Indicators from Mass-Transport Complexes Using 3D Seismic Data. *Mar. Pet. Geology*, 26, 1132–1151. doi:10.1016/j.marpetgeo.2008.09.011
- Canals, M., Lastras, G., Urgeles, R., Casamor, J. L., Mienert, J., Cattaneo, A., et al. (2004). Slope Failure Dynamics and Impacts from Seafloor and Shallow Sub-seafloor Geophysical Data: Case Studies from the COSTA Project. *Mar. Geology*, 213, 9–72. doi:10.1016/j.margeo.2004.10.001

- Chen, H., Xie, X., Guo, J., Su, M., Zong, K., Shang, F., et al. (2015). Provenance of Central Canyon in Qiongdongnan Basin as Evidenced by Detrital Zircon U-Pb Study of Upper Miocene Sandstones. *Sci. China Earth Sci.* 58, 1337–1349. doi:10.1007/s11430-014-5038-6
- Cheng, C., Jiang, T., Kuang, Z., Ren, J., Liang, J., Lai, H., et al. (2021). Seismic Characteristics and Distributions of Quaternary Mass Transport Deposits in the Qiongdongnan Basin, Northern South China Sea. *Mar. Pet. Geology*. 129, 105118. doi:10.1016/j.marpetgeo.2021.105118
- Cook, A. E., Paganoni, M., Clennell, M. B., McNamara, D. D., Nole, M., Wang, X., et al. (2020). Physical Properties and Gashydrate at a Near-Seafloor Thrust Fault, Hikurangi Margin, New Zealand. *Geophys. Res. Lett.* 47, e2020GL088474. doi:10.1029/2020gl088474
- Cox, D. R., Huuse, M., Newton, A. M. W., Gannon, P., and Clayburn, J. (2020). Slip Sliding Away: Enigma of Large sandy Blocks within a Gas-Bearing Mass Transport deposit, Offshore Northwestern Greenland. *Bulletin* 104, 1011–1043. doi:10.1306/10031919011
- Dugan, B. (2012). Petrophysical and Consolidation Behavior of Mass Transport Deposits from the Northern Gulf of Mexico, IODP Expedition 308. *Mar. Geology*. 315–318, 98–107. doi:10.1016/j.margeo.2012.05.001
- Elmore, R. D., Blumstein, R., Engel, M., and Parnell, J. (2003). Palaeomagnetic Dating of Fluid Flow Events along the Moine Thrust Fault, Scotland. *J. Geochemical Exploration* 78–79, 45–49. doi:10.1016/s0375-6742(03)00069-4
- Frey Martinez, J., Cartwright, J., and Hall, B. (2005). 3D Seismic Interpretation of Slump Complexes: Examples from the continental Margin of Israel. *Basin Res.* 17, 83–108. doi:10.1111/j.1365-2117.2005.00255.x
- Gamboa, D., and Alves, T. M. (2015). Three-dimensional Fault Meshes and Multi-Layer Shear in Mass-Transport Blocks: Implications for Fluid Flow on continental Margins. *Tectonophysics* 647–648, 21–32. doi:10.1016/j.tecto.2015.02.007
- Gong, Z. S., and Li, S. T. (1997). *Continental Margin Basin Analysis and Hydrocarbon Accumulation of the Northern South China Sea*. Beijing: Science Press.
- Huang, B., Xiao, X., and Li, X. (2003). Geochemistry and Origins of Natural Gases in the Yinggehai and Qiongdongnan Basins, Offshore South China Sea. *Org. Geochem.* 34, 1009–1025. doi:10.1016/s0146-6380(03)00036-6
- Judd, A. G., and Hovland, M. (2007). *Seabed Fluid Flow: The Impact on Geology, Biology and the marine Environment*. Cambridge: Cambridge University Press.
- Lackey, J., Moore, G., and Strasser, M. (2018). Three-dimensional Mapping and Kinematic Characterization of Mass Transport Deposits along the Outer Kumano Basin and Nankai Accretionary Wedge, Southwest Japan. *Prog. Earth Planet. Sci.* 5, 65. doi:10.1186/s40645-018-0223-4
- Lacroix, B., Travé, A., Buatier, M., Labaume, P., Vennemann, T., and Dubois, M. (2014). Syntectonic Fluid-Flow along Thrust Faults: Example of the South-Pyrenean Fold-And-Thrust belt. *Mar. Pet. Geology*. 49, 84–98. doi:10.1016/j.marpetgeo.2013.09.005
- Lamarche, G., Joanne, C., and Collot, J. Y. (2008). Successive, Large Mass-Transport Deposits in the South Kermadec Fore-Arc basin, New Zealand: the Matakaoa Submarine Instability Complex. *Geochem. Geophys. Geosyst.* 9, Q04001. doi:10.1029/2007gc001843
- Lastras, G., Canals, M., Hughes-Clarke, J. E., Moreno, A., De Batist, M., Masson, D. G., et al. (2002). Seafloor Imagery from the BIG'95 Debris Flow, Western Mediterranean. *Geol* 30, 871–874. doi:10.1130/0091-7613(2002)030<0871:siftbd>2.0.co;2
- Lewis, K. B. (1971). Slumping on a Continental Slope Inclined at 1–4°. *Sedimentology*. 16, 97–110. doi:10.1111/j.1365-3091.1971.tb00221.x
- Li, W., Alves, T. M., Wu, S., Völker, D., Zhao, F., Mi, L., et al. (2015). Recurrent Slope Failure and Submarine Channel Incision as Key Factors Controlling Reservoir Potential in the South China Sea (Qiongdongnan Basin, South Hainan Island). *Mar. Pet. Geology*. 64, 17–30. doi:10.1016/j.marpetgeo.2015.02.043
- Li, X. S., Zhang, Y. Z., Yang, X. B., Xu, X. F., Zhang, J. X., and Man, X. (2017). New Understandings and Achievements of Natural Gas Exploration in the Yinggehai-Qiongdongnan basin, South China Sea. *China Offshore Oil and Gas* 29, 1–11. doi:10.11935/j.issn.1673-1506.2017.06.001
- Liang, C., Liu, C., Xie, X., Yu, X., He, Y., Chen, H., et al. (2020). The Role of Large-Scale Mass Wasting Processes in Changing the Sediment Dispersal Pattern in the Deep-Water Central Canyon of the Northwestern South China Sea. *Mar. Pet. Geology*. 122, 104693. doi:10.1016/j.marpetgeo.2020.104693
- Løseth, H., Gading, M., and Wensaas, L. (2009). Hydrocarbon Leakage Interpreted on Seismic Data. *Mar. Pet. Geol.* 26, 1304–1309. 10.1016/j.marpetgeo.2008.09.008.
- Mao, K., Xie, X., Xie, Y., Ren, J., and Chen, H. (2015). Post-rift Tectonic Reactivation and its Effect on Deep-Water Deposits in the Qiongdongnan Basin, Northwestern South China Sea. *Mar. Geophys. Res.* 36, 227–242. doi:10.1007/s11001-015-9248-x
- Martinsen, O. (1994). “Mass Movements,” in *The Geological Deformation of Sediments*. Editor A. Maltman (London: Chapman & Hall), 127–165. doi:10.1007/978-94-011-0731-0\_5
- Micklethwaite, S. (2008). Optimally Oriented “Fault-valve” Thrusts: Evidence for Aftershockrelated Fluid Pressure Pulses? *Geochem. Geophys. Geosyst.* 9, Q04012. doi:10.1029/2007gc001916
- Moscardelli, L., Wood, L., and Mann, P. (2006). Mass-transport Complexes and Associated Processes in the Offshore Area of Trinidad and Venezuela. *Bulletin* 90, 1059–1088. doi:10.1306/02210605052
- Ogata, K., Pogačnik, Ž., Pini, G. A., Tunis, G., Festa, A., Camerlenghi, A., et al. (2014). The Carbonate Mass Transport Deposits of the Paleogene Friuli Basin (Italy/Slovenia): Internal Anatomy and Inferred Genetic Processes. *Mar. Geology*. 356, 88–110. doi:10.1016/j.margeo.2014.06.014
- Piper, D. J. W., Pirmez, C., Manley, P. L., Long, D., Food, R. D., Normark, W. R., et al. (1997). “Mass-transport Deposits of the Amazon Fan,” in *The Proceedings of the Ocean Drilling Program, Scientific Results*. Editors R.D. Flood, D.J.W. Piper, A. Klaus, and L.C. Peterson (College Station, USA: Ocean Drilling Program), 109–146. doi:10.2973/odp.proc.sr.155.212.1997
- Qin, Z., Wu, S., Wang, D., Li, W., Gong, S., Mi, L., et al. (2015). Mass Transport Deposits and Processes in the north Slope of the Xisha Trough, Northern South China Sea. *Acta Oceanol. Sin.* 34, 117–125. doi:10.1007/s13131-015-0608-9
- Sawyer, D. E., Flemings, P. B., Shipp, R. C., and Winker, C. D. (2007). Seismic Geomorphology, Lithology, and Evolution of the Late Pleistocene Mars-Ursa Turbidite Region, Mississippi Canyon Area, Northern Gulf of Mexico. *Bulletin* 91, 215–234. doi:10.1306/08290605190
- Shipp, R. C., Nott, J. A., and Newlin, J. A. (2004). “Physical Characteristics and Impact of Mass Transport Complexes on deepwater Jetted Conductors and Suction Anchor Piles,” in *Offshore Technology Conference* (Houston, Texas: Extended Abstract), OTC16751. doi:10.4043/16751-ms
- Su, M., Xie, X., Xie, Y., Wang, Z., Zhang, C., Jiang, T., et al. (2014). The Segmentations and the Significances of the central canyon System in the Qiongdongnan basin, Northern South China Sea. *J. Asian Earth Sci.* 79, 552–563. doi:10.1016/j.jseas.2012.12.038
- Sun, Q.-L., Wu, S.-G., Lüdmann, T., Wang, B., and Yang, T.-T. (2011). Geophysical Evidence for Cyclic Sediment Deposition on the Southern Slope of Qiongdongnan Basin, South China Sea. *Mar. Geophys. Res.* 32, 415–428. doi:10.1007/s11001-011-9121-5
- Sun, Q., Alves, T., Xie, X., He, J., Li, W., and Ni, X. (2017). Free Gas Accumulations in Basal Shear Zones of Mass-Transport Deposits (Pearl River Mouth Basin, South China Sea): An Important Geohazard on continental Slope Basins. *Mar. Pet. Geology*. 81, 17–32. doi:10.1016/j.marpetgeo.2016.12.029
- Sun, Q. L., and Alves, T. M. (2020). Petrophysics of fine-grained Mass-Transport Deposits: A Critical Review. *J. Asian Earth Sci.* 192, 10429. doi:10.1016/j.jseas.2020.104291
- Trincardi, F., and Argnani, A. (1990). Gela Submarine Slide: a Major basin-wide Event in the Plio-Quaternary Foredeep of Sicily. *Geo-Marine Lett.* 10, 13–21. doi:10.1007/bf02431017
- Wang, D., Wu, S., Qin, Z., Spence, G., and Lü, F. (2013). Seismic Characteristics of the Huaguang Mass Transport Deposits in the Qiongdongnan Basin, South China Sea: Implications for Regional Tectonic Activity. *Mar. Geology*. 346, 165–182. doi:10.1016/j.margeo.2013.09.003
- Wang, D., Wu, S., Yao, G., and Wang, W. (2015). Architecture and Evolution of Deep-Water Cyclic Deposits in the Qiongdongnan Basin, South China Sea: Relationship with the Pleistocene Climate Events. *Mar. Geology*. 370, 43–54. doi:10.1016/j.margeo.2015.10.002
- Wang, Z., Liu, Z., Cao, S., Sun, Z., Zuo, Q., Wang, Y., et al. (2014). Vertical Migration through Faults and Hydrocarbon Accumulation Patterns in deepwater Areas of the Qiongdongnan Basin. *Acta Oceanol. Sin.* 33, 96–106. doi:10.1007/s13131-014-0579-2

- Wang, Z., Sun, Z., Zhu, J., Guo, M., and Jiang, R. (2015). Natural Gas Geological Characteristics and Great Discovery of Large Gas fields in Deep-Water Area of the Western South China Sea. *Nat. Gas Industry B* 2, 489–498. doi:10.1016/j.ngib.2016.03.001
- Wu, S. G., Yuan, S. Q., Zhang, G. C., Ma, Y. B., Mi, L. J., and Xu, N. (2008). Seismic Characteristics of a Reef Carbonate Reservoir and Implications for Hydrocarbon Exploration in Deep Water of the Qiongdongnan Basin, Northern South China Sea. *Mar. Pet. Geol.* 26, 817–823.
- Wu, W., Li, Q., Yu, J., Lin, C. S., Li, D., and Yang, T. (2018). The central canyon Depositional Patterns and Filling Process in East of Lingshui Depression, Qiongdongnan Basin Northern South China Sea. *Geol. J.* 1, 1–18. doi:10.1002/gj.3143
- Xie, X., Müller, R. D., Ren, J., Jiang, T., and Zhang, C. (2008). Stratigraphic Architecture and Evolution of the continental Slope System in Offshore Hainan, Northern South China Sea. *Mar. Geology.* 247, 129–144. doi:10.1016/j.margeo.2007.08.005
- Zhu, W., Huang, B., Mi, L., Wilkins, R. W. T., Fu, N., and Xiao, X. (2009). Geochemistry, Origin, and Deep-Water Exploration Potential of Natural Gases in the Pearl River Mouth and Qiongdongnan Basins, South China Sea. *Bulletin* 93, 741–761. doi:10.1306/02170908099

**Conflict of Interest:** GY was employed by the company PetroChina Changqing Oil Field Company.

The remaining authors declare that the research was conducted in the absence of any commercial or financial relationships that could be construed as a potential conflict of interest.

**Publisher's Note:** All claims expressed in this article are solely those of the authors and do not necessarily represent those of their affiliated organizations, or those of the publisher, the editors and the reviewers. Any product that may be evaluated in this article, or claim that may be made by its manufacturer, is not guaranteed or endorsed by the publisher.

*Copyright © 2021 Sun, Xie, Wu and Yin. This is an open-access article distributed under the terms of the Creative Commons Attribution License (CC BY). The use, distribution or reproduction in other forums is permitted, provided the original author(s) and the copyright owner(s) are credited and that the original publication in this journal is cited, in accordance with accepted academic practice. No use, distribution or reproduction is permitted which does not comply with these terms.*